# Physicochemical Model for Dose-Dependent Drug Absorption

**J. B. DRESSMAN *x, D. FLEISHER *, and G. L. AMIDON ***

Received July 11, 1983, from *INTERx, Merck Sharp & Dohme Research Laboratories, Lawrence, KS 66044*, and *The University of Kansas, Lawrence, KS 66045*. Accepted for publication October 5, 1983. *Present address: College of Pharmacy, University of Michigan, Ann Arbor, MI 48109.

**Abstract** □ A two-tank perfect-mixing tank model was used to simulate GI absorption. The effect of drug parameters ($pK_a$, solubility, and intrinsic wall permeability) and system parameters (pH profile, volume of intestinal contents, and intestinal flow rate) on drug absorption were studied by numerical data simulation. When the dose did not exceed the solubility of the drug in the intestinal lumen, the fraction absorbed depended on the transit rate relative to the absorption rate and the $pK_a$ relative to the pH profile, but was independent of drug dose. Saturation of one or both tanks led to dose-dependent absorption. The model was used to simulate absorption of chlorothiazide. Good agreement between simulated and experimental data led to the conclusion that the physical characteristics of chlorothiazide, rather than a saturable transport mechanism at the intestinal wall, may be responsible for the dose-dependent absorption observed for this drug. The model was also used to simulate hydrochlorothiazide absorption. By applying the same system parameters used for chlorothiazide, the model simulation correctly predicted the dose proportionality of hydrochlorothiazide absorption. The lack of dose dependency in this case may be attributed to the higher solubility and $pK_a$ of hydrochlorothiazide compared with chlorothiazide.

**Keyphrases** □ Absorption—GI dose-dependent, physicochemical model □ Chlorothiazide—physicochemical model, dose-dependent GI absorption □ Hydrochlorothiazide—physicochemical model, dose-independent GI absorption

Dose-dependent drug absorption is often attributed to absorption *via* a saturable (carrier-mediated) mechanism or to the existence of a so-called absorption window for the drug. In many cases, however, an alternative approach, which takes into account the physical and chemical factors of the drug and GI tract, provides a more reasonable explanation of the observed behavior. Shore *et al.* (1) were the first to recognize the importance of physical parameters to drug absorption in their classical pH-partition hypothesis of GI absorption. They postulated that the rate of absorption is fastest when the drug is in its un-ionized form, with the degree of ionization being a function of pH and, hence, location in the GI tract. Solubility and dissolution rate effects on absorption were studied by Stricker (2, 3) using mechanical *in vitro* systems to simulate absorption. Among his conclusions was the finding that variability in absorption of some sulfonamides could be attributed to their limited and pH-dependent solubilities.

Physiological parameters such as gastric emptying rate may also influence absorption. Clements *et al.* (4) have shown that for drugs, such as acetaminophen, which are poorly absorbed in the stomach, gastric emptying can be the rate-limiting step in absorption. If, in such a case, gastric emptying does not follow a monoexponential relationship, the apparent absorption rate will not be first order, even though the drug is absorbed by passive diffusion. In this report, it is demonstrated that the physicochemical properties of a drug, *i.e.*, its solubility, $pK_a$, and intrinsic absorption rate, can play a significant role in the determination of the relationship between the dose administered and the oral bioavailability. The drugs chosen as examples are chlorothiazide and hydrochlorothiazide. For chlorothiazide, the fraction absorbed orally is known to decrease substantially with increasing dose. By contrast, hydrochlorothiazide exhibits dose-proportional absorption (5–7).

## THEORETICAL SECTION

A two-tank mixing tank model (Fig. 1) provides a simple but useful picture of intestinal absorption. Tank 1 represents the duodenum and, hence, has a smaller volume and lower pH than tank 2, which represents the jejunum and ileum. The following assumptions are incorporated into the model:

1. Absorption from the stomach is minor compared with intestinal absorption. The model could be extended to a three mixing-tank model to accommodate cases in which this assumption is invalid.
2. The drug dose is delivered to the duodenum as a bolus. Dissolution is considered to be instantaneous compared with other processes such as absorption and transit rate. The dissolution rate may, in fact, play an important role in determining the percentage absorbed; its effects will be examined in a future study.
3. Uptake by the intestinal wall is a first-order process which does not involve a saturable carrier mechanism.
4. Absorption of the ionized form is negligible compared with that of the un-ionized form.
5. Transit is a first-order process.

Depending on the drug and the dose administered, three general cases apply:

1. Neither tank becomes saturated after drug is administered.
2. One tank becomes saturated after drug is administered.
3. Both tanks become saturated after drug is administered.

The three cases are illustrated in Figs. 2, 3, and 4, respectively. The basic set of parameters used in the simulations is listed in the *Appendix;* deviations from these values are noted where appropriate in the figure legends. The following symbols are used: $X_{Ti}$, the amount of drug in tank $i$; $V_i$, volume of tank $i$; $f_{ui}$, fraction un-ionized in tank $i$; $Q$, flow or transit rate; $k_{ai}$, intrinsic absorption rate in tank $i$; $X_0$, dose administered; $C_{si}$, saturation concentration in tank $i$; $X_{si}$, $X_{si} = C_{si} \cdot V_i$; $R_i = X_{si}$, apparent absorption rate under saturated conditions in tank $i$; $\tau_1$, time at which $X_{T1} = X_{s1}$; $\tau_{2A}$, time at which $X_{T2} = X_{s2}$ ($X_{T2}$ increasing); and $\tau_{2B}$, time at which $X_{T2} = X_{s2}$ ($X_{T2}$ decreasing).

**Case 1**—In this case, $X_{T1}/V_1$ and $X_{T2}/V_2$ are always less than the saturation concentrations. Loss from tank 1 is given by:

$$-\frac{\partial X_{T1}}{\partial t} = (k_{a1}f_{u1} + Q_1/V_1)X_{T1} \qquad \text{(Eq. 1)}$$

whereas loss from tank 2 is given by:

$$-\frac{\partial X_{T2}}{\partial t} = (Q_2/V_2 + k_{a2}f_{u2})X_{T2} - Q_1X_{T1}/V_1 \qquad \text{(Eq. 2)}$$

Transit out of tank 2 represents drug which is not absorbed, *i.e.*:

$$\frac{\partial X_{t\text{-OUT}}}{\partial t} = Q_2X_{T2}/V_2 \qquad \text{(Eq. 3)}$$

These equations can be solved by using Laplace transforms to yield (for $X_{T1} = X_0$ at $t = 0$):

$$X_{T1} = X_0e^{-At} \qquad \text{(Eq. 4)}$$

$$X_{T2} = \frac{Q_1X_0}{V_1(B-A)}(e^{-At} - e^{-Bt}) \qquad \text{(Eq. 5)}$$

$$X_{t\text{-OUT}} = \frac{Q_2Q_1X_0}{V_2V_1B}\left(\frac{1}{A} + \frac{e^{-Bt}}{B-A} - \frac{Be^{-At}}{A(B-A)}\right) \qquad \text{(Eq. 6)}$$

where $A = k_{a1}f_{u1} + Q_1/V_1$ and $B = k_{a2}f_{u2} + Q_2/V_2$. The fraction of dose absorbed is then given by:

$$F = 1 - \frac{X^{\infty}_{t\text{-OUT}}}{X_0} = 1 - \frac{Q_2Q_1}{V_1V_2(k_{a1}f_{u1} + Q_1/V_1)(k_{a2}f_{u2} + Q_2/V_2)} \qquad \text{(Eq. 7)}$$

This result shows that the fraction absorbed depends on transit rate, intrinsic absorption rate of the un-ionized form, $pK_a$ of the drug, and gastrointestinal pH profile. Variations in transit rate and gastrointestinal pH profile can affect the fraction absorbed in this case, but bioavailability is not dependent on the dose of the drug *per se*.



*0022-3549/84/0900-1274$01.00/0*

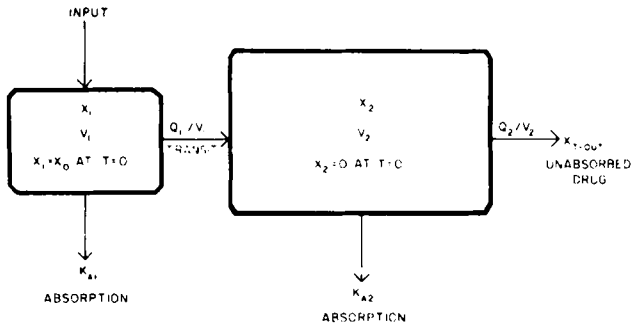


**Figure 1**—*Schematic of the two-tank perfect mixing tank model for oral drug absorption.*

**Case 2**—An example of the case in which one of the tanks becomes saturated occurs when the drug initially saturates tank 1 but levels in tank 2 never reach saturation, *e.g.*, absorption of a poorly soluble weak acid. In this case, it is convenient to split the derivation into two parts: (*a*) from $t = 0$ to $t = \tau_1$, the time at which concentration in tank 1 drops back below saturation, and (*b*) at times longer than $\tau_1$. The second part is essentially described by the equations derived for case 1 by applying the appropriate boundary condition, *i.e.*, $X_{T1}/V_1 = C_s$ at $t = \tau_1$.

Equations for times shorter than $\tau_1$ are:

$$-\frac{\partial X_{T1}}{\partial t} = R_1 + Q_1 X_{T1}/V_1 \qquad \text{(for tank 1)} \qquad \text{(Eq. 8)}$$

$$-\frac{\partial X_{T2}}{\partial t} = -Q_1 X_{T1}/V_1 + (k_{a2} f_{u2} + Q_2/V_2) X_{T2} \text{ (for tank 2)} \qquad \text{(Eq. 9)}$$

$$\frac{\partial X_{t\text{-OUT}}}{\partial t} = Q_2 X_{T2}/V_2 \qquad \text{(for unabsorbed drug)} \qquad \text{(Eq. 10)}$$

Solution of these equations by using Laplace transforms yields:

$$X_{T1} = -\frac{R_1 V_1}{Q_1} + e^{-Q_1 t/V_1}\left(X_0 + \frac{R_1 V_1}{Q_1}\right) \qquad \text{(Eq. 11)}$$

$$X_{T2} = -\frac{R_1}{B} - e^{-Q_1 t/V_1}\left(\frac{R_1 + Q_1 X_0/V_1}{Q_1/V_1 - B}\right) + e^{-Bt}\left(\frac{R_1 + BX_0}{B(Q_1/V_1 - B)}\right)\frac{Q_1}{V_1} \qquad \text{(Eq. 12)}$$

$$X_{t\text{-OUT}} = \frac{-Q_2 R_1 t}{BV_2} + (1 - e^{-Bt})\frac{Q_2}{V_2 B}\left[\frac{Q_1}{V_1 B}\frac{(R_1 + BX_0)}{(Q_1/V_1 - B)}\right] + (e^{-Q_1 t/V_1} - 1)\frac{Q_2 V_1}{V_2 Q_1}\left[\frac{R_1 + Q_1 X_0/V_1}{Q_1/V_1 - B}\right] \qquad \text{(Eq. 13)}$$

$$\tau_1 = \frac{-2.303 V_1}{Q_1}\log\left[\frac{Q_1 X_{s1}/V_1 + R_1}{Q_1 X_0/V_1 + R_1}\right] \qquad \text{(Eq. 14)}$$

The fraction of the dose absorbed can be determined by calculating $\tau_1$ and then evaluating $X^{0\to\tau_1}_{t\text{-OUT}}$ by using Eq. 13 for $t = 0 \to \tau$ and Eq. 3 for $t = \tau_{1\to\infty}$ (solved with initial conditions $X_{T2} = X^{\tau_1}_{T2}$ and $X_{t\text{-OUT}} = X^{\tau_1}_{t\text{-OUT}}$ at $t = \tau_1$, the values of which are found from Eqs. 12 and 13, respectively); that is:

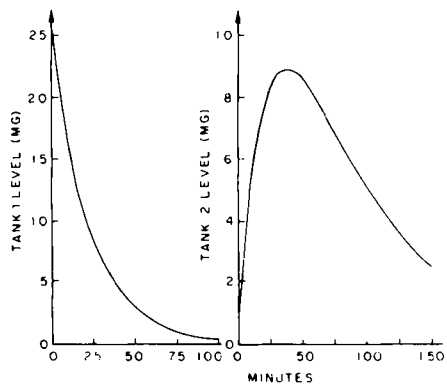


**Figure 2**—*Theoretical levels of drug in tanks 1 and 2 with time after administration of a dose lower than the saturation level in either tank. Case 1 equations apply throughout; the dosage is 25 mg.*

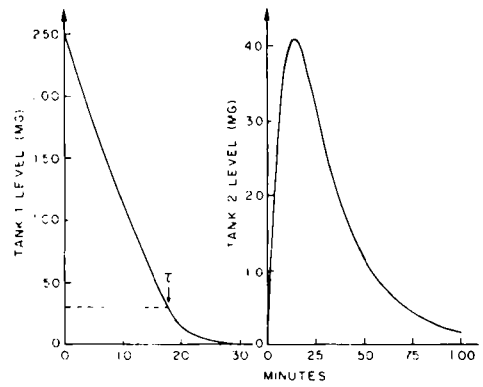


**Figure 3**—*Theoretical levels of drug in tanks 1 and 2 with time after administration of a dose which exceeds the saturation level in tank 1 only ($\tau_1$ = 17.4 min). The intrinsic absorption rate constant is 0.3 min$^{-1}$ for this simulation; the dosage is 250 mg. Case 2 equations apply from* t = 0 *to* t = $\tau_1$.

$$X^{\tau_1\to\infty}_{t\text{-OUT}} = \frac{Q_2 X^{\tau_1}_{T2}}{V_2 B} + \frac{Q_1 X_0 Q_2}{V_1 V_2}\left(\frac{1}{AB}\right) \qquad \text{(Eq. 15)}$$

Then, the fraction absorbed is given by:

$$F_{abs} = 1 - \left(\frac{X^{0\to\tau_1}_{t\text{-OUT}} + X^{\tau_1\to\infty}_{t\text{-OUT}}}{X_0}\right) \qquad \text{(Eq. 16)}$$

Since the term for $X^{0\to\tau_1}_{t\text{-OUT}}$ is a function of the dose administered in addition to the factors listed under case 1, it appears that drugs which exceed their saturation solubilities in the GI tract will exhibit dose-dependent bioavailability. As expected, Eq. 13 indicates that as the dose increases, the fraction absorbed decreases.

**Case 3**—In this case, both tanks achieve levels greater than saturation. Assuming that tank 1 starts out above saturation, the times during which tank 2 becomes saturated ($\tau_{2A} \to \tau_{2B}$) may or may not overlap the time, $\tau_1$, at which tank 1 falls below solubility, as this will depend on the flow rate relative to the absorption rate, solubility at the tank pH values, and the differences in tank volumes.

Differential equations governing drug levels when both tanks are saturated are:

$$-\frac{\partial X_{T1}}{\partial t} = R_1 + Q_1 X_{T1}/V_1 \qquad \text{(Eq. 17)}$$

$$-\frac{\partial X_{T2}}{\partial t} = R_2 + Q_2 X_{T2}/V_2 - Q_1 X_{T1}/V_1 \qquad \text{(Eq. 18)}$$

$$\frac{\partial X_{t\text{-OUT}}}{\partial t} = Q_2 X_{T2}/V_2 \qquad \text{(Eq. 19)}$$

By using the example in which $\tau_{2A} < \tau_{2B} < \tau_1$, the explicit solutions are as follows when $\tau_{2A} < t < \tau_{2B}$:

$$X_{T1} = [\mu(\tau_{2B}) - \mu(\tau_{2A})]\left\{-\frac{R_1 V_1}{Q_1} + e^{-Q_1(t-\tau_{2A})/V_1} \times \left[X_{T1}(\tau_{2A}) + \frac{R_1/V_1}{Q_1}\right]\right\} \qquad \text{(Eq. 20)}$$

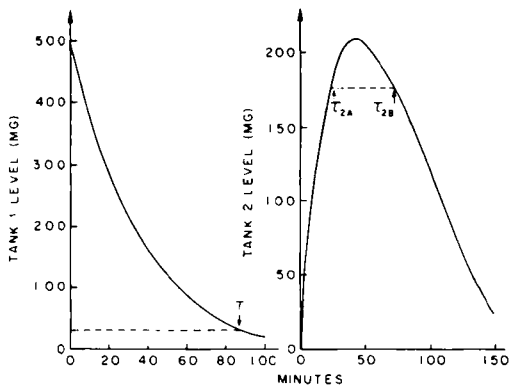


**Figure 4**—*Theoretical levels of drug in tanks 1 and 2 with time after administration of a dose which exceeds the saturation level in both tanks ($\tau_{2A}$ = 23, $\tau_{2B}$ = 71, $\tau_1$ = 87 min). Case 3 equations apply from* t = $\tau_{2A}$ *to* t = $\tau_{2B}$. *For this simulation, the dosage is 500 mg; $pH_2$ = 7.0.*

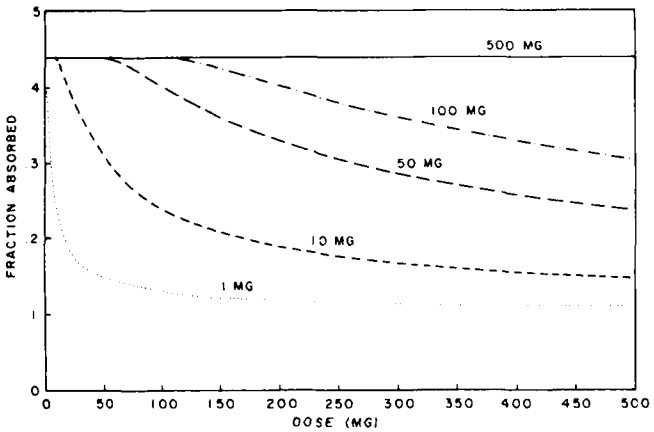


**Figure 5**—*Effect of solubility on the fraction of dose absorbed. Solubilities are expressed as the amount of drug required to saturate tank 1.*

$$X_{T2} = [\mu(\tau_{2B}) - \mu(\tau_{2A})]\left\{\frac{-(R_2 + R_1)V_2}{Q_2} + e^{-Q_1(t-\tau_{2A})/V_1} \times \left[\frac{Q_1 X_{T1}(\tau_{2A})/V_1 + R_1}{Q_2/V_2 - Q_1/V_1}\right] + e^{-Q_2(t-\tau_{2A})/V_2} \times \left[X_{s2} - \frac{Q_1 X_{T1}(\tau_{2A})/V_1}{Q_2/V_2 - Q_1/V_1} - \frac{Q_1 R_1/V_1}{Q_2/V_2(Q_2/V_2 - Q_1/V_1)} + \frac{R_2 V_2}{Q_2}\right]\right\} \quad \text{(Eq. 21)}$$

$$X_{t\text{-OUT}} = [\mu(\tau_{2B}) - \mu(\tau_{2A})]\left\{-(R_1 + R_2)(t - \tau_{2A}) - \frac{Q_2 V_1}{V_2 Q_1}\left[\frac{R_1 + Q_1 X_{T1}(\tau_{2A})/V_1}{Q_2/V_2 - Q_1/V_1}\right][e^{-Q_1(t-\tau_{2A})/V_1} - 1] + [1 - e^{-Q_2(t-\tau_{2A})/V_2}]\left[X_{s2} - \frac{Q_1 X_{T1}(\tau_{2A})/V_1}{Q_1/V_1 - Q_2/V_2} - \frac{Q_1 R_1/V_1}{Q_2/V_2(Q_2/V_2 - Q_1/V_1)} + \frac{R_2 V_2}{Q_2}\right]\right\} \quad \text{(Eq. 22)}$$

where $[\mu(\tau_{2B}) - \mu(\tau_{2A})] = 0$ at $t < \tau_{2A}$, $t > \tau_{2B}$ and 1 for $\tau_{2A} < t < \tau_{2B}$. In this instance, $\tau_{2A}$ is found by substituting $X_{s2}$ for $X_{T2}$ in Eq. 12 and solving for $t$. Similarly, $\tau_{2B}$ is found by substituting $X_{s2}$ for $X_{T2}$ in Eq. 21. At times $\tau_{2B} < t < \tau_1$, case 2 differential equations apply, and at $t > \tau_1$, the system reverts to case 1. A second possible order for $\tau_1$, $\tau_{2A}$, and $\tau_{2B}$ would be $\tau_{2A} < t_1 < \tau_{2B}$. The analogous set of equations for this order of $\tau$ values may be found by applying appropriate initial conditions.

A BASIC program incorporating initial value problem conditions for all possible orders of $\tau_1$, $\tau_{2A}$, and $\tau_{2B}$ and a zero-finding routine to determine the $\tau$ values was used to numerically evaluate the concentration–time profile and fraction absorbed for any given circumstance (see *Appendix*).

## RESULTS AND DISCUSSION

Data were simulated under various conditions for the fraction absorbed *versus* dose plots. To cover the usual dosage range for most drugs, doses of 0–500 mg were studied. Parameters were initially chosen to simulate absorption for a poorly absorbed, weakly acidic drug. The effect of changing each drug and system parameter was then investigated. A discussion of initial parameter choices may be found in the *Appendix*.

**Drug-Related Parameters**—*Solubility*—Figure 5 depicts the influence of drug solubility on the fraction absorbed. For this simulation, solubility refers to the level required to saturate tank 1. For weak acids, tank 1 is saturated at lower levels than tank 2, in which the pH is higher and the volume is larger. Figure 5 shows that the solubility has a very pronounced effect on the relationship between the fraction absorbed and the dose administered. At very high solubility, the fraction absorbed is independent of dose since neither tank becomes saturated. In this case, the fraction absorbed depends on $pK_a$, pH profile, relative absorption, and transit rates but not on dose, since case 1 applies. When the dose exceeds the solubility, case 2 equations apply, and the fraction absorbed varies with dose. The form of the function varies with the drug solubility. The sharpest decrease in the fraction absorbed occurs at doses slightly above the solubility. At doses well above the solubility, the fraction absorbed is low and varies little with dose. Therefore, the dose dependency of absorption depends on the dosage range administered in relation to the solubility. If the doses given are near the solubility, marked dependency of the fraction absorbed on the dose may occur, but if the doses given exceed the solubility by a large amount, absorption will be poor and vary little with dose.

*Drug* $pK_a$—Variation in drug $pK_a$ also causes a large effect on fraction absorbed as a function of dose (Fig. 6). Absorption of weakly acidic drugs with $pK_a$ values ranging from 3.5 to 10.0 was simulated. Simulations indicate that drugs with low $pK_a$ values (3.5 or 4.5) combined with poor intrinsic absorption rates would exhibit very poor absorption from the small intestine, with little dependency on dose. Even though the high pH relative to the drug $pK_a$ ensures adequate solubility, the fraction un-ionized is very low, and so little absorption occurs during the drug residence time. The high solubility in both tanks results in case 1 conditions at all doses studied, which means that the percentage absorbed is independent of dose. Simulations for weaker acids indicate that absorption would be dose dependent in these cases. The fraction absorbed increases with increasing $pK_a$ because the fraction of drug available for absorption, *i.e.*, in the un-ionized form, increases. When the $pK_a$ of the drug is similar to or above the simulated intestinal pH, a high dose relative to the drug intrinsic solubility results in saturation in both tanks and, hence, case 3 equations apply. This occurs for $pK_a = 7.9$ at doses of >275 mg and for $pK_a = 10$ at doses of >225 mg under the conditions chosen (Fig. 6). When both tanks become saturated, the fraction absorbed decreases more rapidly with increasing dose than when only tank 1 is saturated. This is due to the further decrease in fraction available for absorption when both tanks are saturated. Overall, the drug $pK_a$ affects both the form of the fraction absorbed *versus* dose function and the percentage of drug absorbed.

*Intrinsic Absorption Rate Relative to Flow Rate*—Figure 7 shows the impact of changing the ability of the drug to penetrate the membrane relative to the residence time of the drug in the system. The ratio of flow rate to intrinsic absorption rate was varied from 1:1 to 500:1. The absorption rates were chosen to represent a large spectrum of intestinal wall permeabilities. The flow rate was varied from 2 mL/min, which represents an approximate minimum flow in the human jejunum after a meal (8), up to 10 mL/min [maximum flow rate observed in dogs and sheep is ~6 mL/min (9)], thus covering the usual range of physiological values. When the absorption rate is on the same order as the flow rate, the fraction of dose absorbed is very high and virtually in-

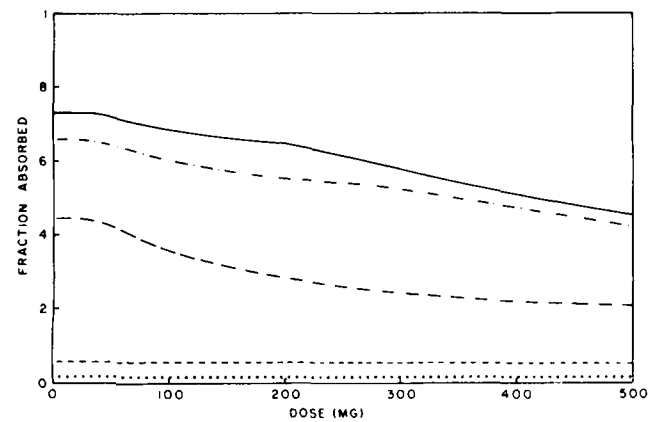


**Figure 6**—*Effect of drug* $pK_a$ *on fraction of dose absorbed. Key to* $pK_a$ *values: (• • •) 3.5; (– – –) 4.5; (— —) 6.7; (• — •) 7.9; (—) 10.0.*

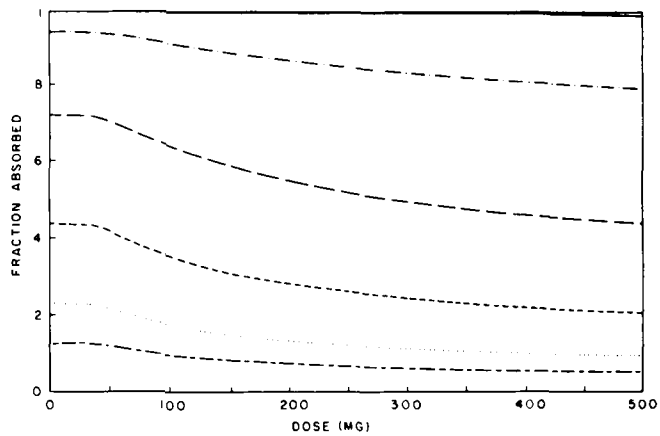


**Figure 7**—*Effect of absorption and transit rate on the fraction of dose absorbed. Key: (• — •)* $Q = 2$ *mL/min,* $k_a = 2$ *min*$^{-1}$*; (— —)* $Q = 2$ *mL/min,* $k_a = 0.2$ *min*$^{-1}$*; (– – –)* $Q = 2$ *mL/min,* $k_a = 0.017$ *min*$^{-1}$*; (• • •)* $Q = 5$ *mL/min,* $k_a = 0.017$ *min*$^{-1}$*; (– — –)* $Q = 10$ *mL/min,* $k_a = 0.017$ *min*$^{-1}$.

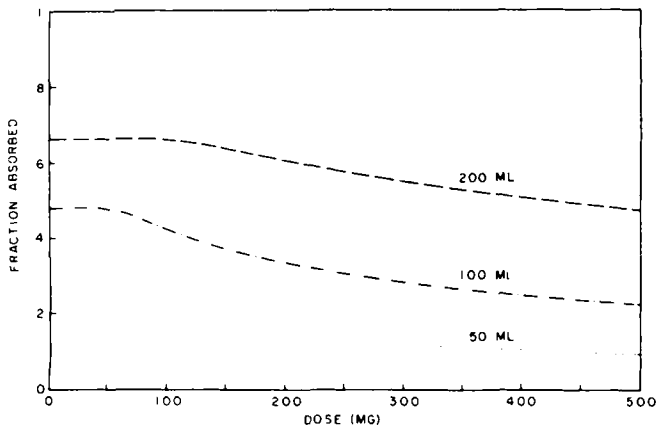


**Figure 8**— *Effect of tank volumes on fraction of dose absorbed. Equal volumes were used in the three simulations.*

dependent of dose. However, when the flow rate is large compared with the absorption rate, absorption is much poorer and more dose dependent. At very high flow rates, the residence time of the drug in the system is too short for extensive drug absorption. In this case, the percentage of dose absorbed is low at all doses and less dose dependency occurs. The major effect of changing the intrinsic absorption rate relative to the flow rate appears to be a shift in the fraction absorbed *versus* dose relationship. At extreme values, the form of the relationship is also affected.

**System Parameters**—*Tank Volumes*—Figure 8 shows the effect of increasing tank volumes on the fraction absorbed *versus* dose relationship. Equal tank volumes were used, ranging from 50 to 200 mL per tank. Increasing the tank volume has two effects. First, the level of drug required to saturate the tank increases. This changes to some degree the range of doses over which dose-dependent absorption occurs. Second, the drug residence time increases, so the drug is available for absorption for a longer period. This causes an upward shift in the fraction absorbed. The combined effect is that increasing the tank volume increases the fraction absorbed and decreases the dependency of absorption on dose. In the analogous *in vivo* situation, ingestion of a large volume of fluid with a poorly absorbed drug may improve the degree of absorption. However, the effect may be attenuated if there is a concomitant increase in flow rate in the intestine.

The effect of changing the relative tank volumes is shown in Fig. 9. Tank volume ratios were varied from 1:1 to 1:10. Although the jejunum is much longer than the duodenum, substantial water reabsorption occurs throughout the upper intestine. Therefore, the relative volume in the duodenum compared with the jejunum is not as low as would be suggested from a purely geometrical calculation. The volume ratios studied reflect these considerations. From the simulations, an increase in the tank volume ratio causes a small vertical shift in the fraction absorbed but has little effect on the shape of the curve. The shift is due to the increase in residence time with increasing total volume. The simulations shown in Fig. 9 all fell in the case 2 category, *i.e.*, only the first tank was saturated. Since the tank 1 volume was held constant, the lack of change in the degree of dose dependency with volume ratio change is reasonable. Overall, changing the relative tank volumes appears to have little

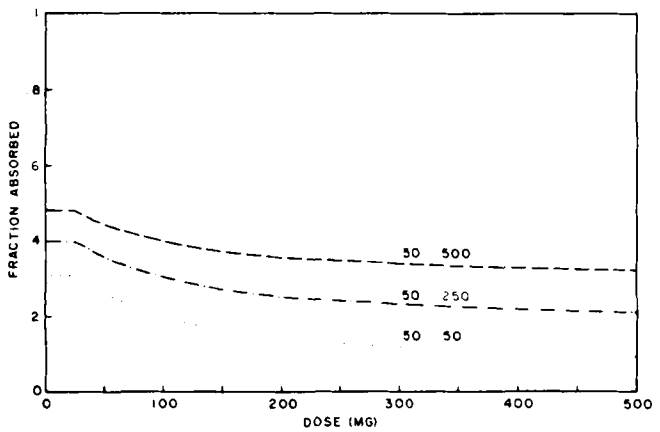


**Figure 9**— *Effect of relative tank volumes on the fraction of dose absorbed. The ratio is shown as tank 1:tank 2.*

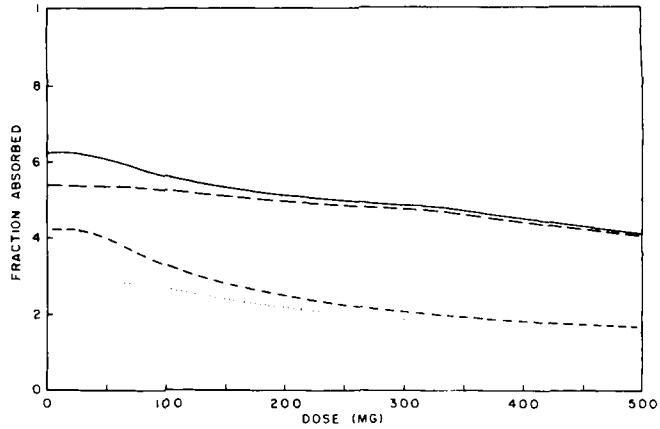


**Figure 10**—*Effect of pH profile on fraction of dose absorbed. Key: (—) $pH_1$ = 5.0, $pH_2$ = 6.7; (— —) $pH_1$ = 6.7, $pH_2$ = 6.7; (- - -) $pH_1$ = 5.0, $pH_2$ = 8.0; (· · ·) $pH_1$ = 6.7, $pH_2$ = 8.0.*

effect on the dose dependency of absorption over a reasonable range of volume ratios.

*pH Profile*—Simulations of drug absorption with several pH profiles are shown in Fig. 10. These represent the range of pH profiles one might reasonably expect to encounter in a normal patient population: low pH (5.0-6.7), high pH (6.7-8.0), flat pH profile (6.7), and sharp pH profile (5.0, 8.0) were simulated at a fixed drug $pK_a$ of 6.7. The pH in tank 1 is the dominant factor in the determination of the shape of the fraction absorbed *versus* dose relationship. Within 2 units of the $pK_a$, the lower the tank 1 pH relative to the $pK_a$, the greater the fraction absorbed. This results from the higher fraction in the un-ionized, absorbable form when the pH is below the $pK_a$. The effect is only significant at doses in the vicinity of the solubility in tank 1 and below, since at high doses the solubility rather than the fraction un-ionized becomes the absorption-limiting factor. The pH in the second tank appears to determine the fraction absorbed. When the pH in tank 2 is similar to the $pK_a$, solubility may be low enough to cause case 3 behavior. When the pH in tank 2 is above the $pK_a$, solubility is higher due to ionization, and case 2 conditions will be operative.

From these simulations it appears that day-to-day and patient-to-patient variation in intestinal pH profile can play a significant role in the determination of the extent of absorption for incompletely absorbed drugs. This explains in part the observation that drugs which are poorly absorbed often exhibit variable absorption.

**Model Assumptions**—The assumptions made in the mixing tank model affect the simulations of the fraction absorbed *versus* dose. For instance, it is assumed that there is bolus delivery to the duodenum and that dissolution is instantaneous in both tanks while the concentration is below saturation. This provides a rather crude approximation of the input and dissolution functions which occur after oral drug administration. Passage of monolithic dosage forms out of the stomach intact would be an example of bolus input, but in most cases, the dosage form breaks up in the stomach so that delivery to the duodenum occurs over an interval of at least several minutes. The dissolution rate may be slow even for dosage forms designed for immediate drug release and particularly so for drugs with low solubility in intestinal fluids. If the dissolution rate is slow compared with the transit rate, absorption will be poorer than predicted by the mixing tank model analysis.

There are three assumptions which pertain to the absorption characteristics of the drug. First, absorption is negligible in the stomach as compared with the small intestine. It has been shown experimentally that for weak acids, such as sulfonamides and barbiturates which would be expected to be relatively well absorbed from the stomach (from pH-partition considerations), absorption occurs 5–10 times faster in the small intestine (10). Second, drug absorption occurs principally in the un-ionized rather than the ionized form. This is the basis of the pH-partition hypothesis (1). Both of these assumptions tend to underestimate the fraction absorbed, since absorption in the stomach or absorption of ionized drug would add to the overall extent of absorption. The third assumption with respect to drug absorption is that the drug is absorbed by a first-order process. First-order absorption applies to a broad range of drugs and is a reasonable assumption in the absence of specific data indicating that a saturable mechanism is in effect.

System assumptions pertain to the selection of values for the pH profile, the volume in the intestine, and the flow rate. The pH profile is constrained by the range of values which occurs physiologically. The volume and flow rate are interrelated. The flow rate in the intestine changes with ingestion of food and fluids, due to changes in gut motility and reabsorption of water. The as-

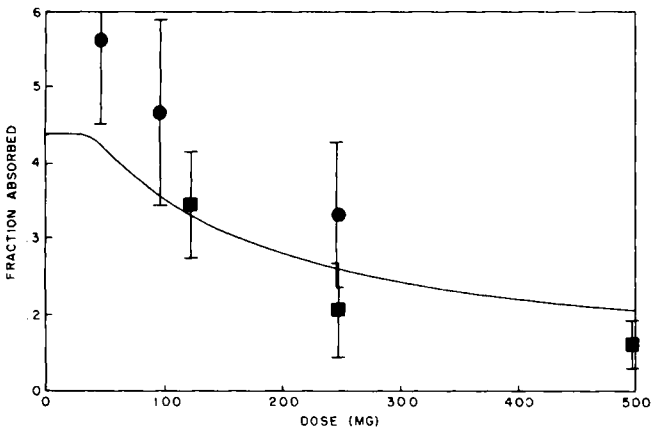


**Figure 11**—*Fraction absorbed* versus *dose simulated for chlorothiazide absorption. Data are taken from Refs. 5 (●) and 6 (■). Error bars indicate standard deviations. The solid line is the simulated data, using parameter values listed in the* Appendix.

sumption that the flow rate is constant throughout the small intestine therefore represents a simplified view of intestinal transit.

**Simulation of Chlorothiazide Oral Absorption** -Figure 11 shows a simulation for oral absorption of chlorothiazide. The selection of parameters used in this simulation is discussed in the *Appendix*. The experimental data were taken from two studies by Welling *et al.* (5, 6) in which solutions of chlorothiazide (prepared with the salt) were administered orally at different dosages. In the first study, doses of 50, 100, and 250 mg were administered. In the second study, the doses were 125, 250, and 500 mg. Although the relationship between the fraction absorbed and dose followed the same form in both studies, the actual extent of absorption seemed to be lower overall in the high-dose-range study, even when the same dosage was administered. The apparent displacement of the results of the second study from those of the first study may partly be explained by a difference in volume and transit rate in the two studies since the fluid intake protocol was not identical in both cases. Meyer and Straughn (11) and Welling and Barbhaiya (12) have shown that increasing the transit time of chlorothiazide in the GI tract, *via* concomitant administration of corn oil emulsion or a meal, resulted in substantial improvement in chlorothiazide bioavailability. A modest increase in fluid intake (12) had only a small effect, however, suggesting that volume/transit rate effects cannot explain all of the difference between the two studies. Comparison of both sets of data with the simulation curve indicates that the form of the fraction absorbed *versus* dose relationship is well described by the mixing tank model. Therefore, the dose-dependent absorption of chlorothiazide may be attributable to solubility ionization-permeability effects rather than a saturable transport mechanism in the intestinal wall. In particular, dose dependency of chlorothiazide may be attributable to limited solubility. Additionally, inspection of the p$K_a$ simulation (Fig. 6) suggests that the low ionization constant is a major limitation to the extent of absorption.

**Simulation of Hydrochlorothiazide Absorption**—Figure 12 shows a simulation for oral absorption of hydrochlorothiazide. System parameters used

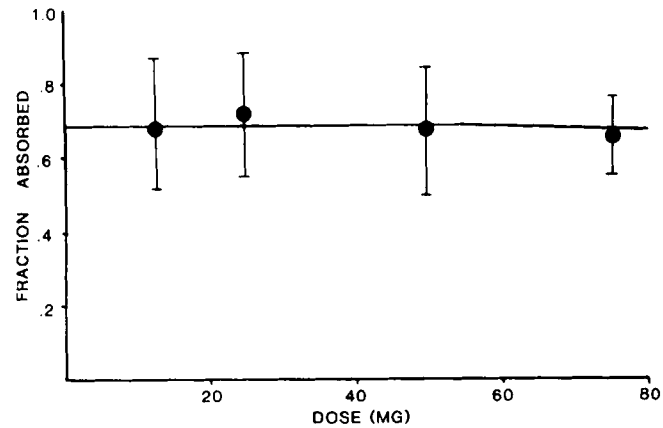


**Figure 12**—*Fraction absorbed* versus *dose simulated for hydrochlorothiazide absorption. Data are taken from Ref. 12. Error bars indicate standard deviations. The solid line is the simulated data, using parameter values listed in the* Discussion *and the* Appendix.

for chlorothiazide were kept the same for hydrochlorothiazide. The drug parameters were changed to literature values of intrinsic solubility (609 mg/L) (13) and p$K_a$ (8.8) (13) and a lower estimate of the absorption rate constant (0.015 $min^{-1}$) to reflect the higher polarity of hydrochlorothiazide. The experimental data were taken from a study of eight subjects by Beerman and Groschinsky-Grind (14). Doses of 12.5, 25, 50, and 75 mg were administered orally. Urinary excretion data indicated that absorption was dose proportional, ~68% of the amount administered at each dose. Simulation of the dose-fraction absorbed relationship using the model correctly predicted the dose proportionality of hydrochlorothiazide absorption.

The difference in absorption behavior of hydrochlorothiazide from that of chlorothiazide is partly attributable to its higher solubility-dose ratio and partly due to the higher p$K_a$. Hydrochlorothiazide is in the un-ionized, absorbable form to at least a 90% extent in both the duodenum and the jejunum, whereas chlorothiazide is mainly in the ionized form at jejunal pH. These factors lead to the higher efficiency of absorption of hydrochlorothiazide that is observed clinically.

## APPENDIX: Numerical Analysis and Parameter Value Selection

Although the initial value problems for cases 1 and 2 are analytically solvable with respect to their individual concentration-time profiles, the determination of $\tau_{2A}$ and $\tau_{2B}$ in case 3 is most conveniently achieved by using a zero-finding routine. In a given trial, the particular case followed depends on the values of the parameters such as solubility, dose, p$K_a$, flow rate, and intrinsic absorption rate of the drug. Also, case switching may occur with time as levels exceed or fall below saturation in the tanks. To accomodate all possibilities, a BASIC program was written that incorporated the three cases and allowed for case switching at $\tau_1$, $\tau_{2A}$, and $\tau_{2B}$. Appropriate initial conditions were set for each case, depending on the order of $\tau_1$, $\tau_{2A}$, and $\tau_{2B}$. It was thereby possible to examine the effects on the concentration-time profile and fraction absorbed for a wide variety of parameter values.

| | | |
|---|---|---|
| System parameters | $V_i$ | volume of tank $i$ |
| | $pH_i$ | pH of tank $i$ |
| | $Q_i$ | flow rate from tank $i$ |
| Derived system parameters | $KT$ | $Q_1/V_1$ |
| | $KE$ | $Q_2/V_2$ |
| Drug parameters | p$K_a$ | |
| | solubility (intrinsic) | |
| Derived drug parameters | $k_{ai}$ | intrinsic absorption rate constant in tank $i$ |
| | $C_{si}$ | total drug solubility in tank $i$ |
| | $f_{ui}$ | fraction un-ionized in tank $i$ |
| Drug variable | $X_0$ | dose |
| Independent variable | $t$ | time |
| Dependent variables | $X_i$ | amount in tank $i$ at time $t$ |
| | $X_{t\text{-OUT}}$ | amount existing unabsorbed at time $t$ |
| Derived variables dictating initial value problem switching | $\tau_1$ | time when $X_1/V_1$ falls below $C_{s1}$ |
| | $\tau_{2A}$ | time when $X_2/V_2$ first exceeds $C_{s2}$ |
| | $\tau_{2B}$ | time when $X_2/V_2$ falls below $C_{s2}$ |
| Derived system/drug parameters | $R_i = k_{ai}f_{ui}C_{si}$ | |

The HP BASIC programs written for an HP 87 system are available on request from the authors. For the simulation of the chlorothiazide dose-dependent absorption, pH, and volumes in the two mixing tanks were chosen to simulate duodenum and jejunum: $pH_1 = 5.5$, $V_1 = 75$ mL; $pH_2 = 7.7$, $V_2 = 150$ mL. This flow rate was 2 mL/min, which is representative of physiological conditions (8). The p$K_a$ [6.7 (15)], solubility [0.4 g/L at pH 4, 0.65 g/L at pH 7 (16)], and the usual range of doses [50 500 mg (5, 6)] were taken from the literature. The intrinsic absorption rate constant (0.017 $min^{-1}$) was estimated on the basis of the effective permeability and the surface area to volume ratio, *i.e.*, $k_{ai} = (SA_i/V_i)\cdot P_{eff}$, where $1/P_{eff} = (1/P_{aq}) + (1/P_w)$. Effective permeability is considered to be a function of the drug and independent of the segment of small intestine under consideration. For chlorothiazide, $P_{eff}$ was estimated to be $7 \times 10^{-5}$ cm/min. The ratio of surface area available for absorption to volume was estimated to be 250, a value between the value calculated on a geometric basis using a filled cylinder model and the value calculated by dividing the estimated total intestinal surface area (including villi surface area) by the cylinder model volume.

These parameter values were also used as a basis for simulations of levels in tanks 1 and 2 in the *Theoretical Section* and for the fraction absorbed *versus*

dose curves in the *Results*. Where other values were used, they are noted in the appropriate figure legends. In the *Results*, values of important drug and system parameters were varied systematically to ascertain their effects on the dose dependency of absorption.

## REFERENCES


(1) P. A. Shore, B. B. Brodie, and C. A. M. Hogben, *J. Pharmacol. Exp. Ther.*, **119**, 361 (1957).

(2) H. Stricker, *Drugs Made Ger.*, **13**, 35 (1970).

(3) H. Stricker, *Drugs Made Ger.*, **14**, 93 (1971).

(4) J. A. Clements, R. C. Heading, W. S. Nimmo, and L. F. Prescott, *Clin. Pharmacol. Ther.*, **24**, 420 (1978).

(5) M. A. Osman, R. B. Patel, D. S. Irwin, W. A. Craig, and P. G. Welling, *Biopharm. Drug. Dispos.*, **3**, 89 (1982).

(6) P. G. Welling, R. H. Barbhaiya, R. B. Patel, T. S. Foster, V. P. Shah, J. P. Hunt, and V. K. Prasad, *Curr. Ther. Res.*, **31**, 379 (1982).

(7) J. E. Baer, H. L. Leidy, A. V. Brooks, and K. H. Beyer, *J. Pharmacol. Exp. Ther.*, **125**, 295 (1959).

(8) H. Davenport, in "Physiology of the Digestive Tract," 4th ed., Yearbook Medical Publishers, Chicago, Ill., 1980, p. 63.

(9) L. Bueno, J. Fioramonti, and Y. Ruckebusch, *J. Physiol.*, **249**, 69 (1975).

(10) W. G. Crouthemal, G. H. Tan, L. W. Dittert, and J. T. Doluisio, *J. Pharm. Sci.*, **60**, 1160 (1971).

(11) M. C. Meyer and A. B. Straughn, *Curr. Ther. Res.* **22**, 573 (1977).

(12) P. G. Welling and R. H. Barbhaiya, *J. Pharm. Sci.*, **71**, 32 (1982).

(13) H. P. Deppeler, in "Analytical Profiles of Drug Substances," Vol. 10, K. Florey, Ed., Academic, New York, N.Y., 1981, p. 405.

(14) B. Beerman and M. Groschinsky-Grind, *Eur. J. Clin. Pharmacol.*, **12**, 297 (1977).

(15) "Martindale: The Extra Pharmacopoeia," 27th ed., A. Wade, Ed., The Pharmaceutical Press, London, 1978, p. xxvii.

(16) "The Merck Index" 9th ed., M. Windholz, Ed., Merck and Co., Rahway, N.J., 1976, p. 277.


# Microcalorimetric Investigation of the Binding of Some Chemotherapeutic Agents and Related Molecules to Calf Thymus DNA


**WILLIAM R. VINCENT *, LEONARD S. ROSENBERG, and STEPHEN G. SCHULMAN ˣ**



Received May 24, 1982, from the *College of Pharmacy, University of Florida, Gainesville, FL 32601.* Accepted for publication January 10, 1983.


*Present address: Arnold & Marie Schwartz College of Pharmacy and Health Science, Long Island University, Brooklyn, NY 11201.



**Abstract** □ Batch microcalorimetry was used to estimate directly the standard enthalpies of the binding of small molecules to DNA. These values were compared with those obtained from spectrophotometric binding constants and van't Hoff plots. The close agreement between the independently obtained enthalpies indicates that the appropriate (best) binding model has four phosphates per binding site. Thermodynamic binding constants were obtained from apparent binding constants measured at different ionic strengths. From these and the measured standard enthalpies, standard free energies and standard entropies of binding were calculated. The weak, presumably external, binding alleged to occur at high formal molar concentration ratios of ligand to DNA bases could not be detected by a measurable heat of binding.



**Keyphrases** □ Microcalorimetry—binding of chemotherapeutic agents and related molecules to calf thymus DNA □ Binding—chemotherapeutic agents and related molecules to calf thymus DNA, microcalorimetry □ DNA—microcalorimetry, binding of some chemotherapeutic agents and related molecules to calf thymus DNA


The binding of certain aromatic cations to nucleic acids for some time has been implicated as a primary process in antibacterial, antiprotozoal, antiviral, mutagenic, and antineoplastic activity (1–7). The changes in the thermal stability and the hydrodynamic and spectroscopic properties of DNA to which aromatic cations are bound have been suggested to indicate that at high ratios of formal DNA base to cation concentrations, intercalation of the flat aromatic portion of the ligand between adjacent base pairs on DNA occurs (8). Intercalation (also called type I binding) entails insertion of the flat aromatic portion of the ligand between base pairs (8–10) or bases (11–12) on DNA, accompanied by a partial unwinding of the double helix. In crystalline samples, X-ray diffraction spectrometry has provided direct evidence for the intercalation of the fungal antibiotic, dactinomycin, between the adjacent base pairs of DNA (13, 14).

The intercalative mode of binding does not appear to extend to all ligand molecules bound to a DNA helix (4). Rather, it is believed that only one molecule of ligand can be accommodated in an intercalative fashion for every four or five phosphate groups of the DNA helix. When nearly all intercalative binding sites of a DNA double helix are occupied, further interaction of the DNA with excess ligand is still able to occur. However, this binding is weaker than the intercalative binding, is not accompanied by hydrodynamic changes in the DNA solutions, and is believed to entail the electrostatic association of the cationic ligands with the anionic phosphodiester linkages at the surface of the helix. This is referred to as external (or type II) binding and occurs in solutions of low DNA base to ligand formal concentration ratios. At high ligand concentrations, some of the larger polycyclic aromatic molecules appear to be bound to the surface of DNA as dimers, because complexes can be spectroscopically distinguished in which there are two ligand molecules bound for each DNA phosphate group (15). The apparent relationship of the reversible reactions of aromatic cations with nucleic acids to the antimicrobial, antineoplastic, and mutagenic activities of the former has resulted in considerable interest in the qualitative and quantitative investigation of these interactions. These studies have usually been concerned with the stoichiometries and formation constants of the complexes formed between the ligands and the nucleic acids (1–22), although more recent work has been centered about the kinetics of binding (16, 21). Techniques such as electronic absorption spectrophotometry, fluorometry, differential spectrophotometry, and circular dichroic spectrophotometry have been employed to determine the amounts of bound and free ligand at each point in the titration of a so-


0022-3549/84/0900-1279$01.00/0